Chapter

LASER-INDUCED BREAKDOWN SPECTROSCOPY: APPLICATION TO POWDER SAMPLES

Hervé K. Sanghapi[1], Krishna K. Ayyalasomayajula[2], Fang Y. Yueh[1,3], Jagdish P. Singh[1,3] and Dustin L. McIntyre[4]

[1]Institute for Clean Energy Technology and
Department of Physics and Astronomy,
Mississippi State University, Starkville, MS, US
[2]Center for Informatics and Analytics,
University of Mississippi Medical Center, Jackson, Mississippi, US
[3]JPS Advanced Technology R&D LLC, Starkville, MS, US
[4]National Energy Technology Laboratory (NETL), Pittsburgh, PA, US

ABSTRACT

Laser-induced breakdown spectroscopy (LIBS) is an atomic emission spectroscopy technique which with the help of a broad band spectrometer can simultaneously perform multi-elemental and *in situ* analysis of various

samples (solid, liquid, powder or gaseous) and various environments which are sometimes difficult to access with standard chemical analytical techniques. In this chapter, we focus on some applications of LIBS on powder samples with varying concentration and how to reduce the matrix effects. By "matrix effect," we refer to the influence of the physical and chemical properties of the sample on the plasma excitation. The possibility of developing a LIBS based sensor system for total carbon quantification in soil samples is discussed and the feasibility of laser-induced breakdown spectroscopy for the analysis of gasification slag is investigated. The results of these two analyses are compared with those obtained from a carbon analyzer and inductively coupled plasma-optical emission spectroscopy (ICP-OES).

THEORETICAL BACKGROUND

LIBS employs a high-energy laser pulse as an excitation source to generate a high-temperature micro-plasma at the target sample through rapid melting and vaporization of the target material [1]. The laser-induced plasma produces both continuum and line emissions. The emission of the continuum radiation (in the spectral range of 2 nm to 600 nm) originates near the sample surface. This continuum results from electron–ion recombination and free–free interactions. Electron-ion recombination gives rise to radiative emission transitions when ions capture an electron with a transition to a bound energy state. Free-free interactions result in free-free emission transitions after loss of kinetic energy by an electron in the field of an ion. The loss of kinetic energy by an electron induces a deceleration of the electron, known as Bremsstrahlung[1,2]. emission. The line emission shows the presence of neutral atoms, ions, electrons and sometimes molecules formed after recombination of the atoms. The plasma center contains the most highly ionized species, while low ionized and neutral species are observed near the outer regions of the plasma plume. The atoms, ions and molecules emit radiation through spontaneous emission of optical wavelength photons as the plasma cools. The spectral analysis of the emitted radiation from a laser-induced plasma will yield both qualitative and quantitative information about the target material's chemical composition. Figure 1.1 shows the schematic diagram of plasma expansion in LIBS [1].

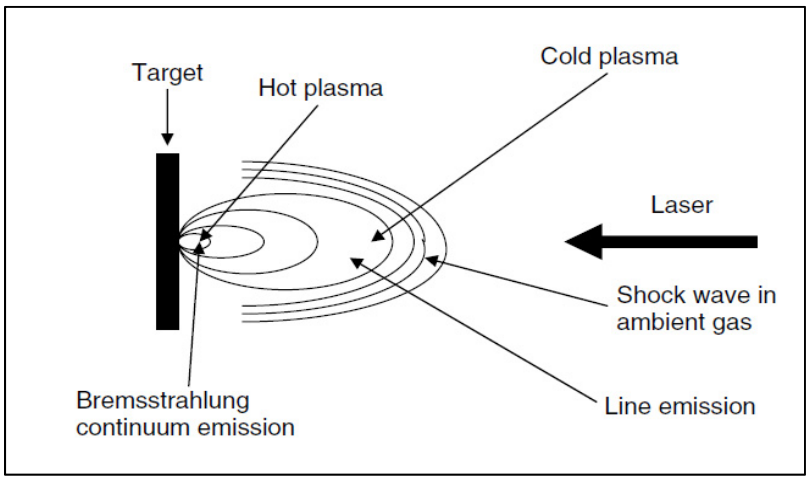

Figure 1.1. Laser-induced plasma expansion in ambient air [1].

Above certain irradiance threshold (typically about 1 GW/cm^2) and depending on the material, the interaction of the laser pulse and the sample eventually causes breakdown in the material. As consequence, some eletrons in the outer shell are ejected and create a vacancy, making the material structure unstable. To restore the stability, electrons from higher orbit farther from the nucleus drop to fill the vacancy. The excess energy in this process as the electrons move between two energy levels emits light at specific wavelength. These emissions, known as optical emission are element-specific and when speactrally resolved, these spectral lines are enough to ascertain the presence of the element in the sample. This approach is called qualitative LIBS analysis and it is a simple and straight forward method. On the other hand, quantitative LIBS analysis is considerably more complicated. Quantitative analysis is often done with calibration LIBS. In this approach, a statistical training model is developed using LIBS spectra from samples of known elemental composition. The compositions of unknown samples are then determined by comparing the LIBS spectra to those of the samples

included in training model. Several different statistical approaches such as simple linear regression (SLR), multivariate data analysis have been used in developing a calibration models. Each approach has its own advantages and disadvantages. The drawback of calibration LIBS is that the accuracy in predicting the composition of unknown sample greatly depends on the composition of known samples included in the training model. The composition of known samples considered in training model must be similar to the composition of unknown samples to achieve accurate predictions [3]. This makes calibration LIBS less flexible, however it is often easier to implement [4].

Although LIBS literature reports detection limits comparable to those of standard analytical techniques such as inductively coupled plasma mass spectrometry, the precision and accuracy of LIBS methods is still influenced by matrix effects and laser-sample interactions [4, 5, 6]. Controllable variables including but not limited to the choice of analytical line, laser pulse energy and detector settings (gate delay and gate width) also affect quantitative analysis of LIBS [7, 8]. Good quantitative results start with the choice of emission lines. The LIBS emission spectrum consists of both continuum and line radiation. Due to the presence of continuum radiation at the very beginning, the detection of emission lines from laser induced plasma is difficult. If the plasma light is integrated over the entire emission time of the plasma, this continuum light can seriously interfere with the detection of weaker emissions from minor and trace elements in the plasma. For this reason, LIBS measurements are usually carried out using time-resolved detection. In this way, the strong white light at early times can be removed from the measurements by turning the detector on after this white light has significantly subsided in intensity but atomic emissions are still present [6]. Figure 1.2 shows the time evolution of continuum and line radiation.

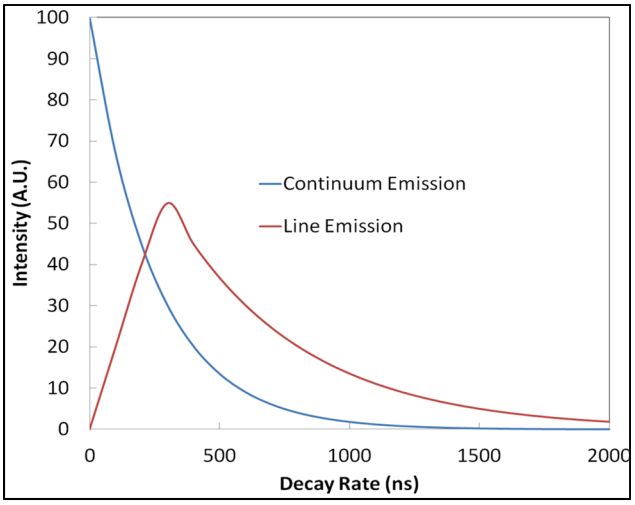

Figure 1.2. Time evolution of continuum and line radiation.

Gate delay (t_d) means time delay between plasma formation and the start of the observation of the plasma light. Gate width (t_w) means time period over which the plasma light is recorded [6]. The t_d and t_w are controlled by using time-resolved detection system in such a way that the continuum emission from the plasma can be gated off and enhancement of signal can be achieved drastically [3].

EXPERIMENTAL DETAILS

Apparatus

Although the experimental setup of LIBS is very simple, it varies from experiment to experiment. In the present chapter, the same setup was used as described below. The schematic diagram of our experimental setup is shown in Figure 1.3. A frequency doubled second harmonic Q-switched Nd: YAG laser (Quantel CFR400 20Hz, 7ns pulse width, 6mm diameter, 235mJ maximum) was used as the excitation source. With availability of only a small amount of the powdered sample, a glass slide with double sided tape

was used on which sample was scattered. The laser was focused onto the sample surface through a 30cm focal length quartz lens and a right angle prism. Spectra were collected with an Andor (Mechelle ME5000) broadband spectrometer (200–975 nm spectral range) through a 100 μm diameter optical fiber equipped with a pickup lens (Ocean Optics Inc. (OOI) Part No.74-UV). The latter was placed 5cm away from the sample and 45^0 with respect to the beam axis. Andor Solis software was used for acquisition setup. The spectrograph signal was integrated with a 1024x1024 intensified charge coupled detector (ICCD). The gate delay and gate width was controlled with the built-in digital delay generator (DDG) of the spectrograph. The DDG is activated by the trigger pulse from the laser Q-switch output to synchronize data acquisition with the laser pulse. The spectrograph was also connected to a personal computer for recording and analyzing data. Samples were mounted on a rotating platform to make sure that each laser pulse hits a fresh spot every time and that data can be collected from various parts of the sample. By collecting data from various part of the sample, the errors due to sample heterogeneity isminimized.

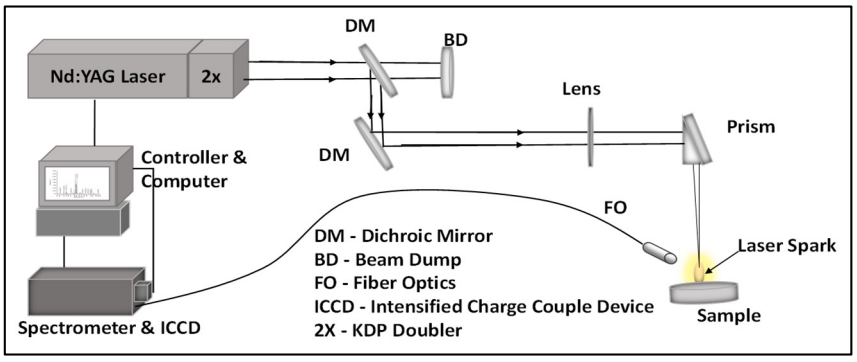

Figure 1.3. Schematic diagram of LIBS experimental setup.

Energy and Temporal Optimization in LIBS

Analytical figures of merit of LIBS measurements depend on laser energy as well as the detection window due to the transient nature of LIBS plasma. Both the laser pulse energy and integration delay has to be optimized for LIBS measurements of a specified sample or experimental setup. In what follows, an example of optimization of experimental parameters such as gate delay and laser pulse energy of our experimental setup is discussed.

Laser Pulse Energy

Laser pulse energy influences the sensitivity of LIBS. The higher the energy, the more the ablated mass is produced which leads to more excited species. Also, the size of the plasma is increased and more excitation of ablated species is observed [5]. Thus, the signal intensity of the spectral line, is increased. However, the increase in laser pulse energy should be controlled in order to avoid saturation and its related effects of self-absorption and self-reversal. A 3D plot is shown in Figure 1.4 to illustrates the variation of intensity of Sr(II) 430.54 nm with respect to laser energy and Sr concentration.

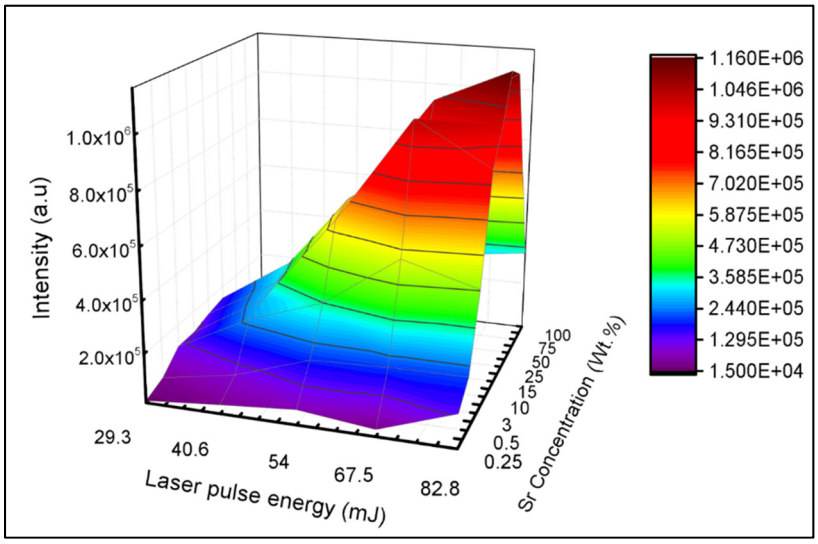

Figure 1.4. 3D variation of intensity with respect to energy and concentration.

In Figure 1.4, we see that the LIBS signal gradually increases with increase of laser energy and becomes almost constant at higher laser energies and in some cases the line intensity drops. The concentration is found to have an effect on the line intensity as well. The LIBS signal increases with an increase of concentration and then considerably drops after 50% concentration. We can then conclude that high laser pulse and high concentration affects the lines intensity. The main reason for the drop in intensity at higher concentration and high laser pulse energy are the saturation and the choice of the emission line notably the use of a resonant line for calibration. Saturation effects invariably lead to the self-absorption and self-reversal. The notion of self-absorption can be connectedto the optical thinness of the plasma. A plasma is said to be optically thin when the emitted light traverses and escapes from the plasma without significant absorption or scattering. When reabsorption is evident, the emitted lines are characterized by a flat-top (evidence of self-absorption) and in some cases a dip at the central frequency is observed as well, and this is referred to as self-reversal. In effect, self-absorption is mostly observed for lines whose lower level transitions are close to the ground state. Because of the strong temperature and electron density gradients, the outer layer of the plasma will be dominated by cool atoms, residing mostly in the ground state. The central core of the plasma will contain a higher density of excited atoms. As these atoms decay to the ground state, the emitted photons close to ground state will have a high probability of being absorbed by the cool atoms in the outer layers, thus reducing the intensity of the emission line [5]. This study indicates that laser pulse energy, approximately 65 mJ is required to obtain reproducible results in LIBS analysis.

Temporal Gating

Because of the high electron density and temperature in the early stage of the laser induced plasma, LIBS spectra are dominated by strong continuum emission that decays faster than spectral lines. This continuum is attributed to Bremsstrahlung (free-free) and recombination (free-bound)

processes. With the Bremsstrahlung process, photons are emitted by accelerated or decelerated electrons in collisions. As for the recombination, a free electron is captured into ionic or atomic energy levels and gives up its excited energy in the form of a photon [6]. In order to retrieve qualitative and quantitative information from the plasma, the recording of the spectra should be delayed from a few nanoseconds to a few microseconds for the continuum emission to drop considerably. As plasma cools down, it is dominated by atomic emission both neutral and ionic species and eventually molecular species. Well resolved spectral lines free of self-absorption can be obtained through temporal gating [9]. Merten et al. reported on the advantages of using gated detector over ungated detector; the gated detector gave a detection limit as low as 0.65 ppm for copper [10]. Comparative studies have been published on the use of ICCD and CCD and their respective influence on improving the quality of LIBS with varying results. Both have their advantages depending on the matrix and spectrometer setup. Although most reported experiment have been performed with ICCD, CCD is more cost effective [11, 12, 13, 14]. The use of a gated detector permits the collection of emission lines with an optimum delay window with good signal-to-background and signal-to-noise ratios. The gated detector is often set by optimizing the detector gate width and gate delay. The influence of these two parameters on the signal has been reported by Sirven [15]. From his studies, signal-to-noise ratio was more influenced by the gate delay than the gate width. The optimum experimental gate delay is obtained by graphing the evolution of the signal-to-background ratio (SBR) and signal-to-noise ratio (SNR) and the gate delay for which the maximum SNR and/or SBR occurs. Plots of the temporal evolution of the SNR and SBR are given in Figure 1.5.

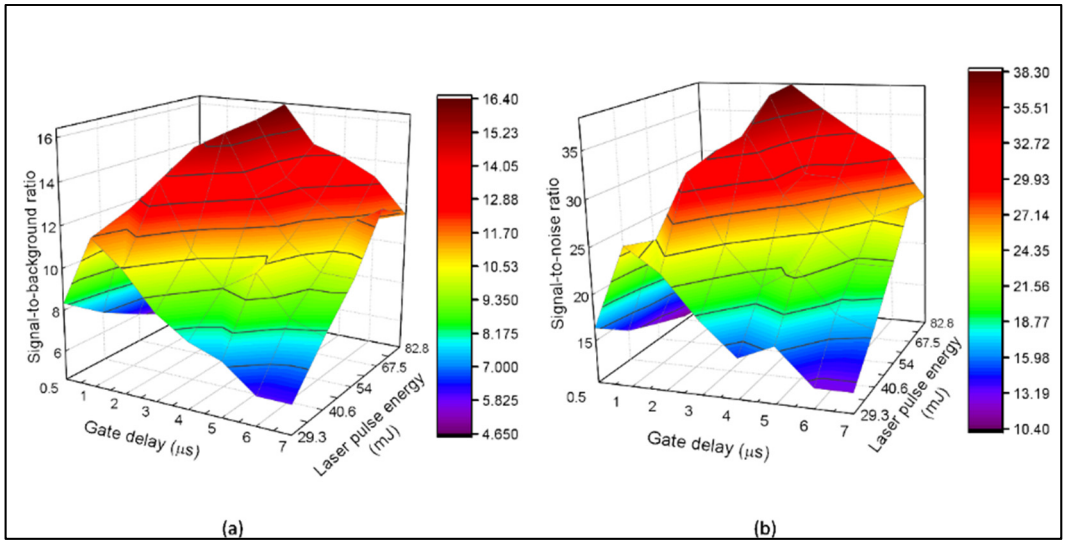

Figure 1.5. 3D plots of (a) Signal-to-background ratio (SBR), (b) signal-to-noise ratio (SNR) of Sr(II) 430.54 nm.

From the above Figures 1.5, SNR and SBR increase with gate delay up to certain value where they start to decrease. A distinction is however observed with respect to the laser pulse energy. At low laser pulse energy, after the maximum ratio is attained, SNR and SBR appreciably decrease whereas at high laser pulse energy, SBR and SNR decrease little after maximum value leading to a kind of plateau implying saturation effects. Measurements within those gate delay windows and laser energy would not be reliable. Also, it is observed that at low gate delay, the SNR and SBR decrease as the laser pulse increases whereas the contrary is observed at longer gate delay. From this, it is suggested that longer gate delay might be compensated for by increasing the laser pulse energy.

Sample Preparation

Despite the versatility of LIBS, its application on direct analysis of powder samples has been a major challenge. Due to the shockwave produced by rapid heating and expansion of plasma, significant amounts of the sample can be blown off. Aslo the particulate nature of the plasma can increase

scattering during irradiation by laser pulses. To overcome such undesirable effects, various sample preparation methods have been proposed. One method is to perform LIBS under low-pressure ambient gas. However, this method has the potential disadvantage ambient gas might denature the powder in the process [16, 17, 18]. Thin films have also been used to prepare powder samples but films can suffer from inhomogeneity [19]. However, most LIBS analysis of powder samples are done with pressed pellets or double-sided tape on a glass slide. Pellets have been extensively used in the literatures [20, 21, 22 23] for analysis of powders. In this method, the sample is mixed with binder, such as polyvinyl alcohol (PVA) and pressed into pellets. However, this technique is limited by the procedure, cost and sometimes the sample available is too small to make a pellet.

On the other hand, the glass slide with double-sided tape is a very simple and cheap sampling method. It consists of applying a piece of double sided tape to a laboratory glass slide and uniformly distributing a small amount of sample onto the exposed side of the tape. Q Sun et al. reported results for samples applied to double-sided tape compared to those obtained by pressing samples into pellets and found no statistical differences between them [24].

Total Carbon in Soil

A soil sample from Starkville, Mississippi, USA was used in this study. The soil sample was finely ground and filtered with a no. 60 sieve. The filtered soil sample was mixed with varying amounts of carbon powder to produce five calibration samples that contained carbon powder concentrations from 3.74% to 9.74%, one sample prepared without mixing any carbon powder and termed as blank, and one unknown sample. The soil sample (5 g) was mixed with 0.4 ml polyvinyl alcohol (2 wt. %. in distilled water) binder. The soil sample was then hand mixed again and placed in a 25 mm–diameter die and pressed into a pellet under 3000 psi. The prepared pellets were placed on a heating plate at 60°C for 90 s to remove the moisture due to the binder. The sample pellets were analyzed in triplicate by a

commercially available carbon analyzer (Leco Truspec, CHN628, USA), and it was found that the total carbon concentration of the blank soil sample, including binder, was approximately 2.43%. The values of 0.5 μs and 5 μs were chosen for the gate delay and gate width respectively. To obtain data with a better signal-to-noise ratio, 10 spectra were collected from each sample and each spectrum recorded was an average of five shots (50 shots total). The triplicate concentrations measured from the carbon analyzer were averaged and considered as a reference while developing the calibration models. The concentration values of the different samples from the carbon analyzer and the contributions of weight from the soil and samples are shown in Table 1.

Table 1. Total Weight Percent of Carbon in the Prepared Pellets

Sample	Carbon analyzer Value (wt. %)	Weight	
		Soil (g)	Carbon powder (g)
blank	2.43±0.05	5	0
1	3.74±0.04	4.9	0.1
2	5.22±0.14	4.8	0.2
3	6.88±0.18	4.7	0.3
4	8.31±0.07	4.6	0.4
5	9.74±0.23	4.5	0.5
Unknown	5.75±0.11	4.75	0.25

Slag Samples

Synthetic slags were prepared by heating reagent grade powders of respective oxides (Al, Ca, Fe, Si and V) at 1425°C for S1 to S7, 1575°C for S8 to S12, and 1500°C for the T1 toT4 series in a 64 mol.% CO_2 – 36 mol.% CO_2 atmosphere for 3 days, followed by water quench. Upon water quenching, all the molten slags were vitrified. Inductively coupled plasma-Optical emission spectroscopy (ICP-OES) analysis was performed after drying the slag samples and grinding them into fine powder, a nominal mass of about 50mg of the sample was fused with ~1g of $Li_2B_4O_7$ and diluted to

a final volume of 100mL using 5% HNO3 [24]. For ICP analysis, spectral lines of Al 309.27 nm, Ca 317.93 nm, Fe 238.20 nm, Si 251.61 nm, and V 292.40 nm were used in this analysis. External calibration and internal standardization procedures [25] were utilized to quantify the analytes and based on the standard reference material (BIR-1) the accuracy of ICP analysis was within ± 7%. For LIBS analysis about 10 mg of the powder sample previously prepared for ICP analysis was placed on a double sided adhesive tape glass slide. All measurements reported herein were carried out with same gate delay (3 μs), gate width (10 μs) and laser pulse energy (67.5 mJ). All spectra correspond to the accumulation of 50 laser shorts with each striking a fresh surface by rotating the sample. The elemental composition of slag sample is listed in Table 2.

Table 2. Concentration ranges of analytes in slag samples analyzed by ICP-OES

Sample (wt%)	Al	Ca	Fe	Si	V
S1	14.12	6.01	4.85	29.62	0.01
S2	10.55	6.26	2.64	35.11	0.93
S3	23.86	6.05	5.37	21.66	0.01
S4	9.66	6.01	2.54	31.97	2.90
S5	13.69	6.19	1.60	26.37	3.69
S6	15.10	5.61	2.57	22.49	6.38
S7	14.19	7.21	1.44	34.15	3.29
S8	12.49	5.84	2.21	31.71	0.01
S9	25.69	6.86	3.07	24.38	0.02
S10	25.95	7.42	4.51	24.24	6.07
S11	17.32	5.89	3.27	24.12	1.61
S12	19.03	6.60	3.05	25.55	4.19
T1	24.14	5.23	13.86	53.39	0.03
T2	20.93	5.09	12.45	47.07	10.97
T3	17.51	5.08	11.39	39.92	23.04
T4	9.68	5.25	8.32	27.28	46.65
T5	6.49	5.18	6.72	19.72	59.35

Data Analysis

Simple linear regression (SLR), multiple linear regression (MLR) and partial least squares regression (PLS-R) are used for quantitative analysis of slags and total carbon in soil. The SLR assumes a linear relationship between the peak intensity (area) of the analyte line and the elemental concentration. However, instead of using the individual analyte lines as a function of the elemental concentration to calibrate the SLR model, ratios of the analyte lines to other present elements as a function of the concentrations were used to negate the interference effects. This method is known as internal standardization. The MLR model was also evaluated for LIBS calibration to account for various interference effects caused by other components of the sample matrix or random experimental errors. The MLR uses more analyte lines to produce the calibration data and was found by previous researchers to perform much better than the SLR [27]. The MLR calibration curve was obtained by fitting the linear equation below to a set of experimental data consisting of the ratio of the measured peak areas of C and Fe and the known concentrations of carbon. The MLR procedure estimates a linear equation of the form

$$C_p = b_0 + \sum_i^n (b_i A_i) \quad (1)$$

where, C_p is the concentration of the carbon in the pellet, b_0 is the intercept, b_i is the coefficient corresponding to A_i, and A_i is the ratio of peak areas of the C and Fe lines. Multiple lines can be used in the regression to improve the measurement accuracy by correcting for the matrix effect. The predictive quality of the calibration models was evaluated by calculating the correlation coefficient R^2 and relative accuracy. The relative accuracy (RA%) is calculated as follows:

$$RA(\%) = \frac{|C_{libs} - C_{true}|}{C_{true}} \times 100\% \quad (2)$$

where, C_{libs} is the value from the LIBS measurement and C_{true} is the known value.

An alternative means of minimizing the interference effects caused by other components of the sample matrix, is the use of multivariate analysis like PLS-R. In effect, PLS-R has been widely used to minimize the matrix effect [28, 29, 30]. PLS provides a model for the relationship between a set of predictor variables X (n objects, m variables) and a set of response variables Y (n objects, p response). In this case, the m variables are the LIBS spectra intensities and the p responses are properties such as the concentration. The p response has to be independently measured for each sample. If the spectral data contain information about the properties of interest, a reliable calibration model can be constructed [31]. The samples with known elemental concentrations are used to create a model relating Y to X that is used to predict the concentrations of unknown specimens. The Unscrambler X version 10.3 (Camo Software Inc, Woodbridge NJ, USA), OriginPro 2015 (OriginLab Corporation, Northampton MA, USA), Veusz1.23.1 (Jeremy Sanders) and excel software were used for data analysis.

RESULTS AND DISCUSSION

Plasma Characterization

In order to retrieve qualitative and quantitative information from collected spectra, the plasma should satisfy certain conditions. Principally, it should be optically thin, in local thermodynamic equilibrium (LTE) and stoichiometric [6]. LIBS plasma is often characterized by parameters such as the electron temperature and electron number density within the limits of local thermodynamic equilibrium. Various methods of obtaining plasma temperature and electron number density can be found in Singh and Thakur [1]. Plasma characterization reported here are with respect to the slag analysis. In Figure 1.6, Boltzmann plot method was used to determine the electron plasma temperature. Calcium lines were used so that electron impact parameter could be referred from Griem [33]. in the calculation of the electron density. The lines Ca(II) 396.84 nm, Ca(I) 430.25 nm and Ca(I)

443.49 nm used are reported in Table 3. The temperature obtained was T_e= 5994±280 K. Different ionization levels were used in order to avoid lines with close excitation energy. This is to limit the effect of varying spectral response of the apparatus, as well as to minimize the sensitivity to small fluctuations in emission intensity [32]. Electron density of laser-induced plasma ranges from 10^{16} to 10^{19} cm^{-3}. The reported electron density was determined from Stark broadening [31]. The spectral line of Ca (422.67 nm) was fitted using a Lorentzian profile while the corresponding broadening coefficient at T=5000 ºK was considered from Griem [33]. An average electron density N_e of $9.87x10^{17}cm^{-3}$±4.67% and $9.01x10^{17}cm^{-3}$±6.84% was observed for all samples.

Table 3. Spectroscopic data of calcium for slag plasma

Lines (nm)	g_iA_{ij} ($x10^8s^{-1}$)	E_i - E_j (eV)	X_z (eV)	K_B (eVK^{-1})	w (nm)
Ca(II) 396.84	0.7	0 - 3.12	6.11	$8.62x10^{-5}$	
Ca(I) 422.67	6.54	0 - 2.93			$4.84x10^{-4}$
Ca(I) 430.25	2.72	1.89- 4.78			
Ca(I) 443.49	1.34	1.88- 4.68			

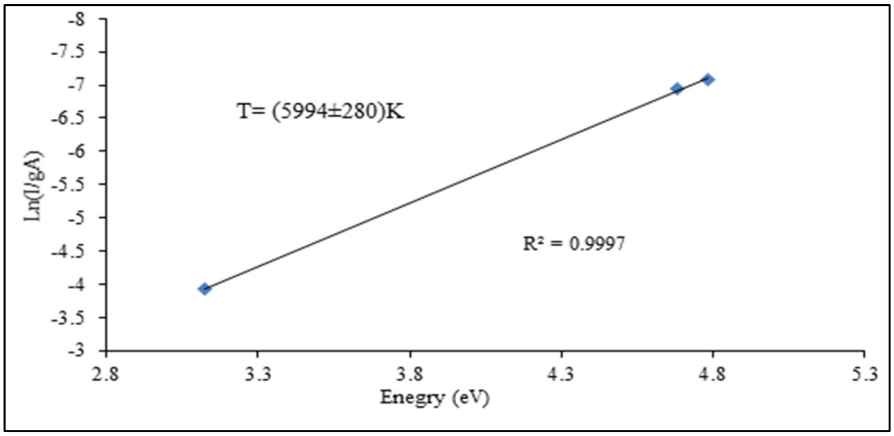

Figure 1.6. Boltzmann plot for electron plasma temperature.

QUANTITATIVE ANALYSIS

Case of Slags

Precise and accurate quantitative results of LIBS analysis are limited by the so-called matrix effect [12, 17]. Kraushaar et al. [34] observed that major elements in slag vary in a range of at least 10% (relative) and that these variations of analyte concentrations contribute to matrix effects. These observed variations ultimately affect the ablation rate thus increasing the fluctuation in the emission lines and reducing the sensitivity of the instrument. Many studies have investigated matrix effects and its possible remedies are using internal standards and multivariate analysis (MVA) [34, 35, 36, 37]. In this study, internal standardization is used for univariate calibration with Ca and Si as internal standards whereas PLS-R calibration models are used for MVA by considering the spectral range for each element (Al, Ca, Fe, Si and V). Most results reported here are based on the first set of samples (S1 to S12). In order to confirm the trend of our results, a second set of samples (T1 to T4) with a different concentration range was used. Ten samples from set S were used for calibration and two for predictions. For set T, since only five sample are available, four were used for calibration and one for predictions.

Univariate Simple Linear Regression (SLR)

Univariate calibration curves for the two sets of data are shown in Figure 1.7 where intensity ratios are plotted against concentration ratios. Ca and Si were used as internal standards. The correlation coefficients R^2 range between 0.969 and 0.993. A reduced number of samples were observed for vanadium in order to obtain better linear regression curves. Only six out of ten samples from set S were used for V, while ten and nine were used for Ca and Si respectively and eight for both Al and Fe. The reduction of the number of samples used in the calibration can be attributed to the presence of outliers and the difficulties in minimizing shot to shot fluctuations in multi-elemental analysis.

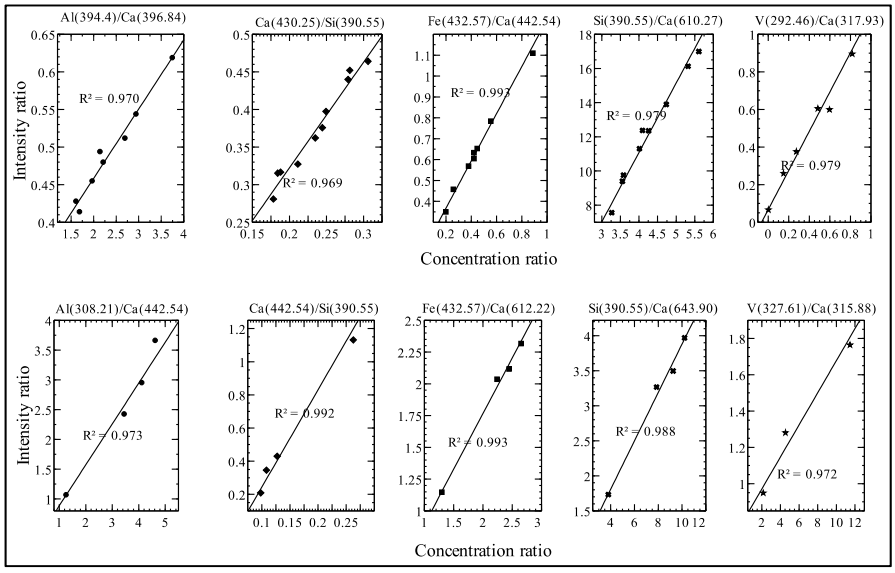

Figure 1.7. Simple linear calibration plots. Sample set S (Top) and Sample set T (Bottom).

Multivariate Partial Least Squares Regression (PLS-R)

Figure 1.8 shows the PLS-R calibration models for Al, Ca, Fe, Si and V. It is observed that the R^2 values are almost equal to 1, revealing a strong correlation between the predictions and references. With slopes tending to 1 and validation (val) R^2 close to the calibration (cal) R^2, we can qualify this model as good enough for running our regression. Furthermore, calibration and validation best fits deviate very little from target line due to high value of R^2. Likewise, in the SLR, a reduced number of samples for the PLS-R of V is also observed.

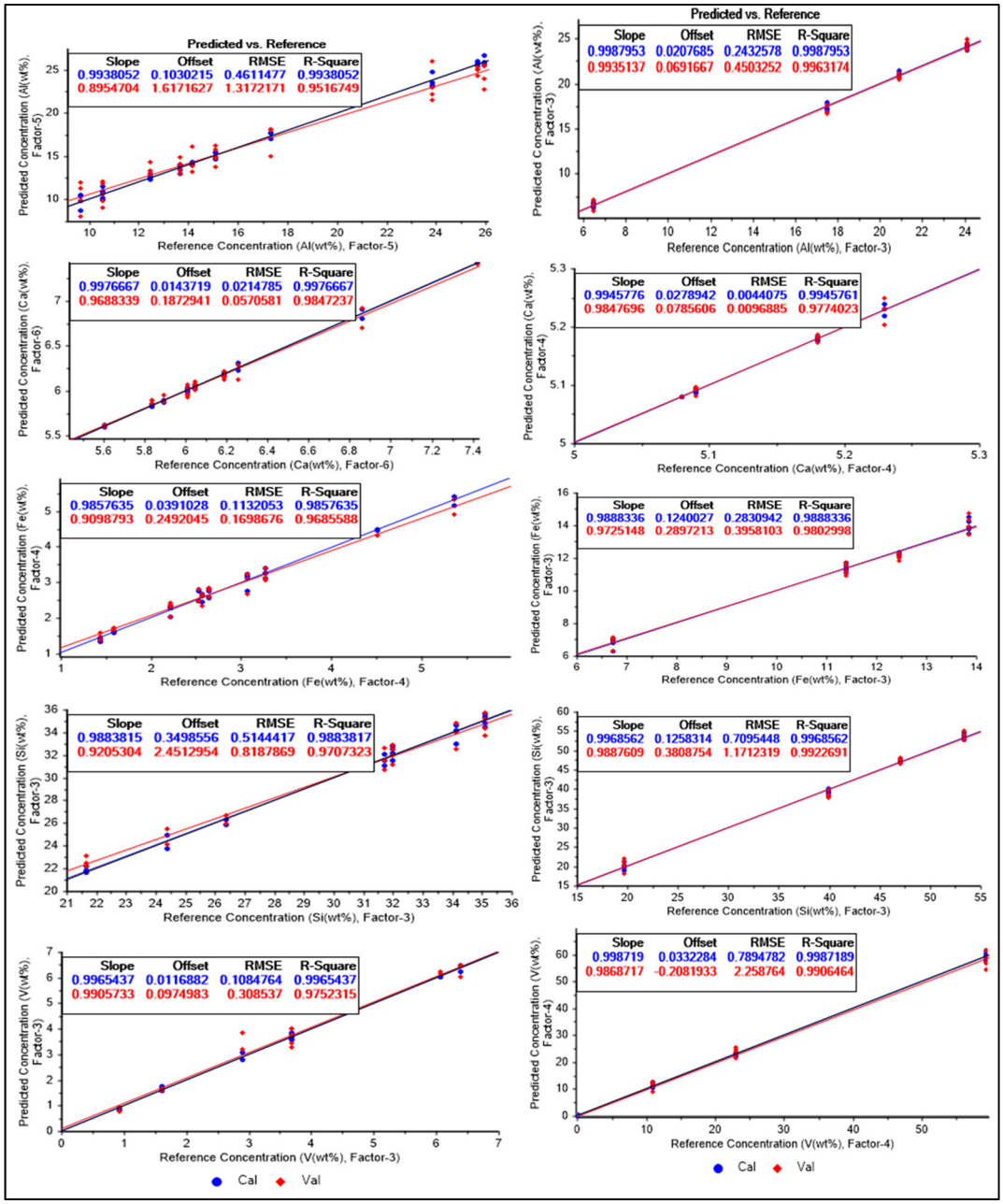

Figure 1.8. Partial least squares regression calibration curves. Sample set S (Left) and Sample set T (Right).

Analytical Figures of Merit

To evaluate the figures of merit of LIBS measurements, predictive results from these two approaches are compared to those obtained by ICP-OES. Measurement precisions and percent accuracy error are evaluated. An approximation of the detection limits were calculated.

Comparative Results of Partial Least Square, Univariate Calibration Curves versus ICP

Here, LIBS results are reported and compared to ICP. Predictions were done with sample S1, S7, S12 and T4. LIBS measurements were performed with SLR and PLS-R and reported as the mean value of five measurements. In general, the repeatability for the major elements in terms of relative standard deviation (RSD) outlined in Table 2 for SLR and PLS-R are consistent except for Al and Ca. In terms of accuracy, the percent accuracy error (Table 4) explains the deviation from the reference values.

Table 4. Comparative LIBS and ICP results

	LIBS	LIBS	ICP	% Accuracy Error		Confidence & Significance level		
	(SLR)	(PLS)				(95%, 0.05)		
wt%				SLR	PLS	t Statistic	DF	P value>|t|
Al_S12	18.96±1.98	18.99±0.17	19.03	0.35	0.19	0.03		0.976
Ca_S1	6.13±0.28	6.01±0.05	6.01	2.03	0.06	1.12		0.327
Fe_S1	5.16±0.20	4.78±0.26	4.85	6.44	1.53	2.11		0.102
Si_S1	30.18±1.77	29.14±1.86	29.62	1.86	1.63	1.21		0.293
V_S12	3.27±0.39	3.26±0.13	4.19	21.95	22.2	0.05		0.962
Al_T4	11.21±2.10	10.11±0.20	9.68	15.83	4.4	1.26		0.277
Ca _T4	5.39±0.34	5.12±0.07	5.25	2.58	2.57	1.94		0.125
Fe_ T4	13.96±1.47	8.08±0.32	8.32	13.72	2.84	9.33		0.001
Si_ T4	27.22±3.74	21.18±3.74	27.28	0.24	17.96	2.22		0.09
V_ T4	37.85±10.49	36.67±8.84	46.65	18.87	21.38	0.2		0.854

From Table 4, the accuracy error of both quantitative approaches is within almost the same ranges (0.35-21.95%) for SLR and (0.06-22.2) for PLS-R. To compare the two analitycal approaches used, a paired-sample t-test was performed within the 95% confidence level and significance level of 0.05 with results shown in Table 4 to find the significance of the difference of the population (number of measurements) means using SLR and PLS-R. The null hypothesis was ($mean_{(SLR)}$ - $mean_{(PLS-R)}$ =0). For the overall results, at the 0.05 significance level, the difference of the population means was not significantly different from the test difference (0) as the p-values (Table 4) were greater than 0.05. This signifies that no appreciable statistical difference was observed using univariate SLR calibration with internal standard and the multivariate PLS-R except for Ca (S12), Fe (S12), Fe (T4) and V (S7). Using the reference values and the accuracy error to interpret the p-values for these, SLR performed better than PLS_R on Ca (S12) and Fe (S12) while PLS_R performed better than SLR on Fe (T4). As for V (S7) the paired-sample test could not be validated based on the high accuracy error with respect to the reference value. With the exception of V for which the accuracy error is about ±20% the reference value, variations observed are linked to the nature of the slag itself where concentration variations increase matrix effects; the use of internal standard and multivariate analysis have resulted in LIBS measurements for other elements with slight variation from ICP results. Simultaneous use of univariate calibration curves with internal standard and PLS regression in multi-elemental matrix demonstrates the capability of LIBS as an alternative technique for analyzing gasification slags.

Limit of Detection

The limit of detection (LOD) can be calculated from a spectrum with lowest analyzed concentration where (LOD) is defined as $3CN/I$. N being the noise calculated from the standard deviation of the background near the analyzed line; C is the concentration of the analyzed line; I is the intensity

of the analyzed line. Estimated limits of detection of Al, Ca, Fe Si and V are reported in (Table 5).

Table 5. Estimated limit of detection

Elements (S Sample)	LOD (wt %)	Elements (T Sample)	LOD (wt %)
Al(396.15)	0.167	Al(394.4)	1.31
Ca(430.25)	1.201	Ca(442.54)	0.78
Fe(432.57)	0.171	Fe(432.57)	1.92
Si(390.55)	0.243	Si(390.55)	10.36
V(292.46)	-	V(327.61)	-

Case of Total Carbon in Soil

The LIBS spectra of pelletized soil samples were recorded using various experimental conditions such as lens-to-sample distance, laser energy per pulse, gate delay, gate width, and sample rotation speed, which were all determined to be optimal for this study. These parameters were optimized to achieve the best signal-to-noise ratio and lowest possible relative standard deviation.

Simple Linear Regression (SLR)

Due to the spectral interference of the carbon line at 247.88 and Fe emission lines at 247.86nm and 247.95nm, the carbon line at 193.03nm have been used by Da Silva et al. [38] who reported this strong interference with Fe emission lines. If the selected analyte line has spectral interference due to overlapping or self-absorption, the correlation between the line intensity and analyte content will be overly complicated. In this study, the wavelength range of the spectrograph is from 200 nm to 975 nm. Due to this limitation of the spectrometer, the carbon line at 193.03 nm could not be used; therefore, the carbon line at 247.88 nm was used instead. To account for

interference with Fe emission lines, a different approach to the SLR method was applied. The total peak area under C 247.88 nm and Fe 247.99 nm was considered as a single peak area for C 247.88 nm and used in the analysis. The ratio of total peak area of C 247.88 nm with that of Fe 246.51 nm and Fe 247.48 nm (as a function of carbon concentration measured from the carbon analyzer) was used to develop the calibration curves. The peak area of each selected line was extracted from the spectral data of each pellet sample with the aid of a function provided in the Andor iStar software. Figure 1.9 shows the carbon pellet spectra of the present study and confirms the same choice for calibration.

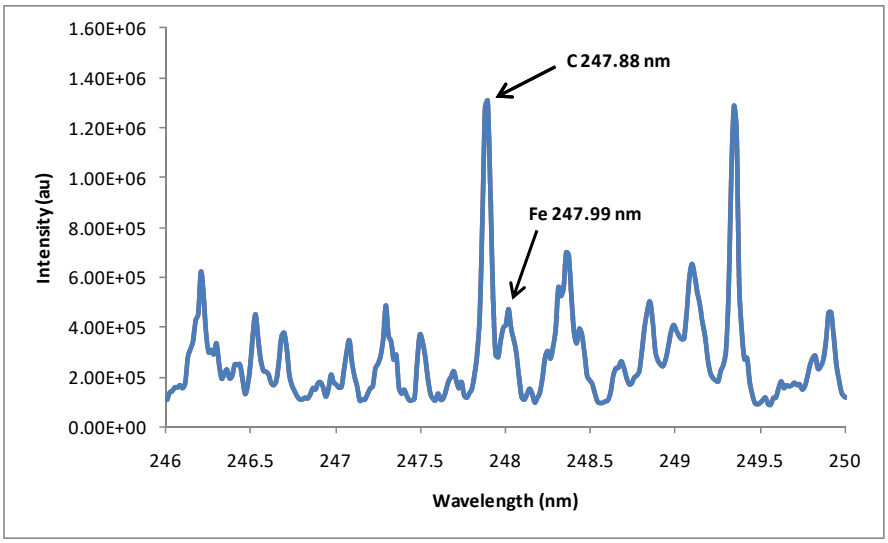

Figure 1.9. Spectrum of emission lines selected for LIBS analysis of total carbon.

The LIBS data were collected on six samples that varied in carbon concentration from 2.43% to 9.74% to develop the calibration curves. The data from the 9.74% sample shows a lower intensity ratio value as well as strong saturation effects due to the high concentration of carbon. Zhang et al. [39] investigated the carbon concentration effects and reported that the intensity of the analyte line with higher carbon concentration emitted a much higher intensity than those of the lower concentrations. The calibration curve with the 9.74% sample data produced poor results due to the strong

saturation and self-absorption effects. To improve the calibration results, the 9.74% sample was omitted from the data and the calibration curves were developed from the remaining samples (2.43% to 8.31%). Figure 1.10 shows the calibration curves for carbon using the SLR method; the error bars represent a single standard deviation.

The correlation coefficients of the ratio of the C 247.88 nm line with the Fe 246.51 nm and Fe 247.48 nm lines were 0.996 and 0.993 respectively. The calibration data from both the C247/Fe246 and C247/Fe247 line ratios were used to predict the concentrations of the validation data. The uncertainties and RA% were calculated and are reported in Table 6 for comparison.

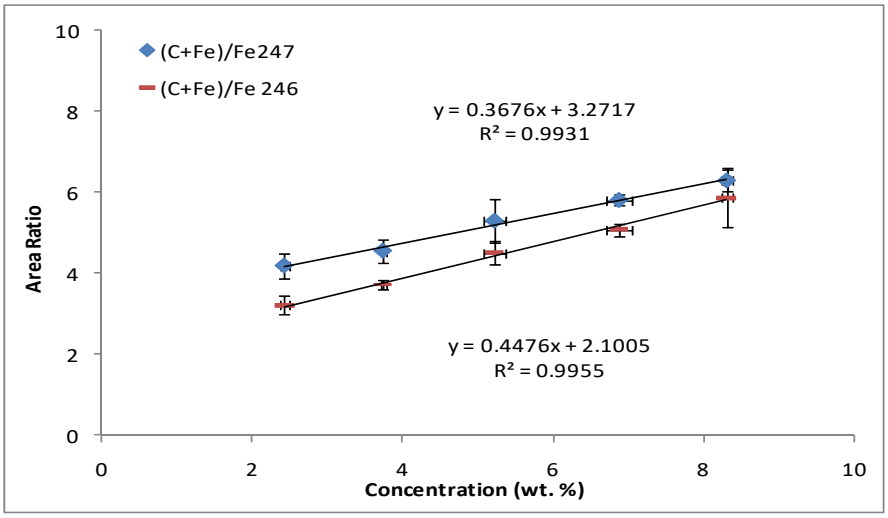

Figure 1.10. Calibration plots based on line-intensity.

Even though the R^2 values of the SLR method with the ratio of both the Fe lines are almost the same, the uncertainty, here evaluated as the relative accuracy (RA) is used to select the best ratio lines. From Table 6, the ratio of the C 247.88 nm line with the Fe 246.51 nm line has an overall uncertainty better than that of the ratio of the C 247.88 nm line with the Fe 247.48 nm line for the validated data. Therefore, the calibration data for the C 247.88–to–Fe 246.51 nm ratio was used for the analysis of an unknown sample. Data

was normalized to further improve the reproducibility of LIBS measurement and overcome effects such as shot-to-shot plasma variations. The absolute line intensities of all the C and Fe lines were normalized with the total plasma emission using the function provided by the Andor iStar software. However, there was no change in the SLR calibration data results.

Table 6. Comparison between LIBS Analysis (SLR model) and Carbon Analyzer Data

Sample	C analyzer value (wt. %)	LIBS value (wt. %)			
		C 247/Fe 246	RA%	C 247/Fe 247	RA%
blank	2.43±0.05	2.49±0.44	2.41	2.56±1.24	5.44
1	3.74±0.04	3.76±0.42	0.58	3.70±1.91	1.19
2	5.22±0.14	5.40±0.69	3.31	5.26±1.85	0.76
3	6.88±0.18	6.53±0.49	4.98	7.02±0.95	2.12
4	8.31±0.07	8.50±0.84	2.33	8.74±3.68	5.22

Multiple linear regression (MLR)

To better account for effects such as saturation, interference, and random experimental errors, the MLR technique was employed. MLR can be a good approach to predict the unknown concentration if the elemental concentration can be well correlated with the intensity of a few spectral lines. However, this method can be inefficient or inappropriate if many spectral lines are needed or if there is significant collinear relation between the spectral lines. Therefore, the selection of analyte lines when employing the MLR is very important [27, 40, 41]. To avoid such setback in our analysis, the ratio of C 247.88 nm lines with Fe lines (246.51 and 247.48 nm) was selected for the linear regression. The correlation coefficient obtained was 0.996 and uncertainty and RA% values for validation data using the MLR model are given in Table 7 for comparison.

Table 7. Comparison between LIBS Analysis (MLR model) and Carbon Analyzer Data

Sample	C Analyzer Value (wt.%)	LIBS Value (wt.%)	RA%
blank	2.43±0.05	2.54±0.43	4.47
1	3.74±0.04	3.55±0.62	5.14
2	5.22±0.14	5.13±0.55	1.72
3	6.88±0.18	6.96±0.31	1.28
4	8.31±0.07	8.38±0.70	0.86

Results, reported with Carbon Analyser and LIBS are expressed as the measured values ± the uncertainty. The uncertainty and RA% values from MLR model for most of the samples improved when compared to the SLR model output. The ability of LIBS to produce accurate quantitative data with the calibration models was tested by examining the LIBS spectra of an unknown sample under the same experimental conditions. The uncertainty and RA% value for the unknown sample when using the SLR method with a ratio of the Fe 246.51 nm lines and MLR calibration methods were acceptable and within their limit.

Comparative Results of LIBS and C Analyzer

The calibration results for the unknown sample for both the SLR and MLR models are reported in Table 8 for comparison.

Table 8. Comparison between LIBS Analysis of SLR and MLR Models and Carbon Analyzer Analysis for Unknown Sample

C Analyzer Value (wt. %)	SLR		MLR	
	Value (wt. %)	RA%	Value (wt. %)	RA%
5.75±0.11	5.50±0.71	4.26	5.34±0.51	7.10

The MLR model provided better uncertainty and RA% results for most of the samples used for the validation data as compared to the SLR model.

In the case of the unknown sample, the MLR model gave better uncertainty values than the SLR model. The accuracy of the MLR model can depend on the analyte lines and combination of lines chosen; the best results for the available lines are reported here.

CONCLUSION

In this chapter, spectrochemical analyses of gasification slags and total carbon in soil using laser-induced breakdown spectroscopy have been discussed. The powder samples were prepared using pellets and double-sided tape on glass slide. In the case of measuring total carbon, quantitative analyses were performed using simple linear regression (SLR), multiple linear regression (MLR) and results compred with those of a Carbon Analyzer. Simple linear regression (SLR) and partial least square regression (PLS-R) were used for slags and results compared with those of ICP-OES. Internal standard was used in univariate (SLR) calibration curves to minimize the shot to shot variation in plasma. The correlation coefficient is often the first parameter used to evaluate how two entities relate. The higher (above 0.90) this correlation coefficient, the stronger their interrelation. However, this is just a necessary but not sufficient condition. Although the calibration curves in this study give correlation coefficients greater than 0.95, it is worth performing predictions and evaluating the accuracy error in order to draw further conclusion of the methods used. From the slag analysis, the paired-sample t-test within the 95% confidence level yielded p-values greater than 0.05, meaning no appreciable statistical difference was observed between the SLR with internal standard and the multivariate PLS-R for most of the analytes. It follows that in LIBS analysis, besides its inherent dependence on experimental setup, quantitative results also depend on the element of interest, the choice of the selected lines and the data analysis approach. Thus, the simultaneous use of univariate calibration curves with internal standard (intensity ratio) and PLS-R in multi-elemental analysis can help reduce the matrix effect of slags associated to their high variation in concentration. The results also show that LIBS can be successfully applied to quantitative measurement of total carbon in soil with a relative accuracy

better than 5%. The MLR model gave better uncertainty values for most of the samples in comparison.

REFERENCES

[1] J. P. Singh and S. N. Thakur, *Laser-induced breakdown spectroscopy*. Elsevier, 2007.

[2] A. Miziolek, V. Palleschi, and I. Schechter, *Laser Induced Breakdown Spectroscopy: Fundamentals and Applications*. Cambridge University Press, 2006.

[3] K. K. Ayyalasomayajula, "Laser spectroscopy for material characterization : Chemical analysis using Laser-Induced Breakdown Spectroscopy (LIBS)," PhD dissertation, Mississippi State University, 2014.

[4] L. Alm, "Development of Laser-Induced Breakdown Spectroscopy for Analyzing Rinds and Layered Structures in Martian Rocks," Ms thesis, Luleå University of Technology, 2011.

[5] D. Cremers and L. Radziemski, *Handbook of Laser–Induced Breakdown Spectroscopy,* 2nd ed. John Wiley & Sons, 2013.

[6] A. Miziolek, V. Palleschi, and I. Schechter, *Laser Induced Breakdown Spectroscopy: Fundamentals and Applications*. Cambridge University Press, 2006.

[7] X. L. Mao, M. a. Shannon, A. J. Fernandez, and R. E. Russo, "Temperature and Emission Spatial Profiles of Laser-Induced Plasmas during Ablation Using Time-Integrated Emission Spectroscopy," *Appl. Spectrosc.*, vol. 49, no. 7, pp. 1054–1062, Jul. 1995.

[8] I. Bassiotis and A. Diamantopoulou, "Effects of experimental parameters in quantitative analysis of steel alloy by laser-induced breakdown spectroscopy," ... *B At. Spectrosc.*, vol. 56, no. 6, pp. 671–683, Jun. 2001.

[9] B. T. Fisher, H. a. Johnsen, S. G. Buckley, and D. W. Hahn, "Temporal Gating for the Optimization of Laser-Induced Breakdown

Spectroscopy Detection and Analysis of Toxic Metals," *Appl. Spectrosc.*, vol. 55, no. 10, pp. 1312–1319, Oct. 2001.

[10] J. a Merten, E. Ewusi-Annan, B. W. Smith, and N. Omenetto, "Optimizing gated detection in high-jitter kilohertz powerchip laser-induced breakdown spectroscopy," *J. Anal. At. Spectrom.*, vol. 29, no. 3, p. 571, 2014.

[11] M. Sabsabi, R. Héon, and L. St-Onge, "Critical evaluation of gated CCD detectors for laser-induced breakdown spectroscopy analysis," *Spectrochim. Acta - Part B At. Spectrosc.*, vol. 60, no. 7–8, pp. 1211–1216, 2005.

[12] J. E. Carranza, E. Gibb, B. W. Smith, D. W. Hahn, and J. D. Winefordner, "Comparison of nonintensified and intensified CCD detectors for laser-induced breakdown spectroscopy.," *Appl. Opt.*, vol. 42, no. February, pp. 6016–6021, 2003.

[13] M. Mueller, I. B. Gornushkin, S. Florek, D. Mory, and U. Panne, "Approach to Detection in Laser-Induced Breakdown Spectroscopy," *Anal. Chem.*, vol. 79, no. 12, pp. 4419–4426, 2007.

[14] H. Heilbrunner, N. Huber, H. Wolfmeir, E. Arenholz, J. D. Pedarnig, and J. Heitz, "Comparison of gated and non-gated detectors for double-pulse laser induced plasma analysis of trace elements in iron oxide," *Spectrochim. Acta - Part B At. Spectrosc.*, vol. 74–75, pp. 51–56, 2012.

[15] J. B. Sirven, P. Mauchien, and B. Sallé, "Analytical optimization of some parameters of a Laser-Induced Breakdown Spectroscopy experiment," *Spectrochim. Acta - Part B At. Spectrosc.*, vol. 63, no. 10, pp. 1077–1084, 2008.

[16] H. Suyanto, H. Kurniawan, T. J. Lie, and K. Kagawa, "Application of laser plasma confinement and bending effect for direct analysis of powder sample," *Spectrochim. Acta Part B …*, vol. 57, no. 8, pp. 1325–1332, Aug. 2002.

[17] N. Idris, K. Kagawa, F. Sakan, K. Tsuyuki, and S. Miura, "Analysis of Heavy Metal Pollution in Soil Using Transversely Excited Atmospheric CO2 Laser-Induced Plasma by Trapping the Soil in

Microstructured Holes on Metal Subtargets," *Appl. Spectrosc.*, vol. 61, no. 12, pp. 1344–51, Dec. 2007.

[18] Z. Lie, M. Pardede, and R. Hedwig, "Spectrochemical analysis of powder using 355 nm Nd-YAG laser-induced low-pressure plasma," *Anal. Bioanal. Chem.*, vol. 390, no. 7, pp. 1781–1787, Apr. 2008.

[19] R. Hedwig and W. Budi, "Film analysis employing subtarget effect using 355 nm Nd-YAG laser-induced plasma at low pressure," *Spectrochim. Acta - Part B At. Spectrosc.*, vol. 61, no. 12, pp. 1285–1293, Dec. 2006.

[20] K. Y. Yamamoto, D. A. Cremers, M. J. Ferris, and E. F. Foster, "Detection of Metals in the Enviroment Using a Portable Laser-Induced Breakdown Spectroscopy Instrument," *Appl. Spectrosc.*, vol. 50, no. 2, pp. 222–233, 1996.

[21] R. A. Multari, L. E. Foster, D. A. Cremers, and M. J. Ferris, "Effect of sampling geometry on elemental emissions in laser-induced breakdown spectroscopy," *Appl. Spectrosc.*, vol. 50, no. 12, pp. 1483–1499, 1996.

[22] P. Fichet, P. Mauchien, and C. Moulin, "Determination of impurities in uranium and plutonium dioxides by laser-induced breakdown spectroscopy," *Appl. Spectrosc.*, vol. 53, no. 9, pp. 1111–1117, 1999.

[23] B. Sallé, D. A. Cremers, S. Maurice, R. C. Wiens, and P. Fichet, "Evaluation of a compact spectrograph for in-situ and stand-off Laser-Induced Breakdown Spectroscopy analyses of geological samples on Mars missions," *Spectrochim. Acta - Part B At. Spectrosc.*, vol. 60, no. 6, pp. 805–815, 2005.

[24] Q. Sun, M. Tran, B. W. Smith, and J. D. Winefordner, "Determination of Mn and Si in iron ore by laser-induced plasma spectroscopy," *Anal. Chim. Acta*, vol. 413, no. 1–2, pp. 187–195, May 2000.

[25] J. C. Jain, C. R. Neal, and J. M. Hanchar, "Problems Associated with the Determination of Rare Earth Elements of a 'Gem' Quality Zircon by Inductively Coupled Plasma-Mass Spectrometry," *Geostand. Newsl.*, vol. 25, no. 2–3, pp. 229–237, 2001.

[26] M. A. Schneegurt, J. C. Jain, J. A. Menicucci, S. A. Brown, K. M. Kemner, D. F. Garofalo, M. R. Quallick, C. R. Neal, and J. F. Kulpa,

"Biomass byproducts for the remediation of wastewaters contaminated with toxic metals," *Environ. Sci. Technol.*, vol. 35, no. 18, pp. 3786–3791, 2001.

[27] K. K. Ayyalasomayajula, V. Dikshit, F. Y. Yueh, J. P. Singh, and L. T. Smith, "Quantitative analysis of slurry sample by laser-induced breakdown spectroscopy.," *Anal. Bioanal. Chem.*, vol. 400, no. 10, pp. 3315–3322, Jul. 2011.

[28] J. Amador-Hernández, "Partial least squares regression for problem solving in precious metal analysis by laser induced breakdown spectrometry," *J. Anal. At. Spectrom.*, vol. 15, no. 6, pp. 587–593, 2000.

[29] S. Clegg, E. Sklute, and M. Dyar, "Multivariate analysis of remote laser-induced breakdown spectroscopy spectra using partial least squares, principal component analysis, and related techniques," *Spectrochim. Acta - Part B At. Spectrosc.*, vol. 64, no. 1, pp. 79–88, Jan. 2009.

[30] S. Laville, M. Sabsabi, and F. R. Doucet, "Multi-elemental analysis of solidified mineral melt samples by Laser-Induced Breakdown Spectroscopy coupled with a linear multivariate calibration," *Spectrochim. Acta Part B At. Spectrosc.*, vol. 62, no. 12, pp. 1557–1566, Dec. 2007.

[31] M. Z. Martin, N. Labbé, T. G. Rials, and S. D. Wullschleger, "Analysis of preservative-treated wood by multivariate analysis of laser-induced breakdown spectroscopy spectra," *Spectrochim. Acta Part B At. Spectrosc.*, vol. 60, no. 7–8, pp. 1179–1185, Aug. 2005.

[32] E. Tognoni, V. Palleschi, M. Corsi, G. Cristoforetti, N. Omenetto, I. Gornushkin, B. W. Smith, and J. D. Winefordner, "From sample to signal in laser-induced breakdown spectroscopy: a complex route to quantitative analysis," in *Laser-Induced Breakdown Spectroscopy (LIBS)*, A. Miziolek, V. Palleschi, and I. Schechter, Eds. Cambridge University Press, 2006, pp. 122–170.

[33] H. Griem, *Spectral line broadening by plasmas*. Academic Press, New York, 1974.

[34] M. Kraushaar, R. Noll, and H. U. Schmitz, "Slag analysis with laser-induced breakdown spectrometry.," *Appl. Spectrosc.*, vol. 57, no. 10, pp. 1282–1287, Oct. 2003.

[35] C. Chaleard, P. Mauchien, and N. Andre, "Correction of Matrix Effects in Quantitative Elemental Analysis With Laser Ablation Optical Emission Spectrometry," *Journal of Analytical Atomic Spectrometry*, vol. 12, no. 2. pp. 183–188, 1997.

[36] J. Vrenegor, R. Noll, and V. Sturm, "Investigation of matrix effects in laser-induced breakdown spectroscopy plasmas of high-alloy steel for matrix and minor elements," *Spectrochim. Acta Part B At. Spectrosc.*, vol. 60, no. 7–8, pp. 1083–1091, Aug. 2005.

[37] J. A. Aguilera, C. Aragón, V. Madurga, and J. Manrique, "Study of matrix effects in laser induced breakdown spectroscopy on metallic samples using plasma characterization by emission spectroscopy," *Spectrochim. Acta Part B At. Spectrosc.*, vol. 64, no. 10, pp. 993–998, Oct. 2009.

[38] R. M. da Silva, D. M. B. P. Milori, E. C. Ferreira, E. J. Ferreira, F. J. Krug, and L. Martin-Neto, "Total carbon measurement in whole tropical soil sample," *Spectrochim. Acta Part B At. Spectrosc.*, vol. 63, no. 10, pp. 1221–1224, 2008.

[39] Q. Zhang, J. Zhang, L. Zhang, X. Li, Q. Guo, and G. Fu, "Signal enhancement of the laser-induced plasma in the soil mixed with carbon," *Chinese Sci. Bull.*, vol. 55, no. 4–5, pp. 386–389, 2010.

[40] H. K. Sanghapi, K. K. Ayyalasomayajula, F. Y. Yueh, J. P. Singh, D. L. McIntyre, J. C. Jain, and J. Nakano, "Analysis of slags using laser-induced breakdown spectroscopy," *Spectrochim. Acta B.* 115, 40-45 (2016).

[41] K.K. Ayyalasomayajula, F. Y. Yueh, J. P. Singh, D. L. McIntyre, and J. C. Jain. "Application of laser-induced breakdown spectroscopy for total carbon quantification in soil samples," *App. Opt.* 51(7): 149–154 (2012).